

NANOCOMPOSITE OF Ag⁰NPs SUPPORTED ON SiO₂ MICROSPHERES INDUCES WOUND HEALING IN EXPERIMENTAL SKIN INCISIONS

I. YAÑEZ-SÁNCHEZ^a, F. J. GÁLVEZ-GASTELUM^b, C. VELÁSQUEZ-ORDOÑEZ^a, M. I. MANZO-RIOS^b, F. ROJAS-GONZALEZ^c, M. A. GARCÍA-SÁNCHEZ^c, J. J. SÁNCHEZ-MONDRAGÓN^d, M. L. OJEDA-MARTÍNEZ^{a*}

^a*Nanoscience and Nanotechnology Research Center, Department of Natural and Exact Sciences, CUValles, University of Guadalajara*

^b*Pathology Laboratory, Department of Microbiology and Pathology, CUCS, University of Guadalajara*

^c*Department of Chemistry, Autonomous Metropolitan University-Iztapalapa, P.O. Box 55-534, México D.F. 09340*

^d*National Institute of Astrophysics, Optics and Electronics (INAOE) Luis Enrique Erro No. 1, Tonantzintla, Puebla, México C.P. 72840*

We investigated the influence of coverage the surface of silica microspheres with silver nanoparticles (Ag⁰NPs) in to skin wound healing. We prepared silica microspheres, either pristine or doped with Ag⁰NPs that were created after the hydrolysis/condensation of tetraethoxysilane, according to Stöber methodology; these substrates were characterized through spectroscopic and microscopic techniques. The wound healing activity was tested and monitored on male Wistar rats (n=15) during 12 days. Finally, a skin biopsy samples were analyzed through hematoxylin-eosin and Masson-trichrome stainings or by immune histochemical localization of fibroblastic and proliferative cells markers. Silica microspheres of 300 nm in size, carrying Ag⁰NPs of about 1.6-3 nm were synthesized and employed for skin tissue repairing. The animals that received treatment with pristine or Ag-doped silica nanosystems showed similar recovery patterns; nevertheless, the animals treated with Ag doped microspheres exhibited additional features such as an enlarged presence of hair follicles, insignificant inflammatory infiltrate and an epithelial thickness of a lesser extent. Similarly, in the same group an important presence of blood microvessels, fibroblast and proliferating cells were observed. These results suggest that silica microspheres coated with Ag⁰NPs induce significantly better skin wound reparation effects through the modulation of angiogenic, inflammatory, fibrogenic, and proliferative mechanisms.

(Received December 6, 2017; Accepted February 6, 2018)

Keywords: Wound healing, Ag-nanoparticles, SiO₂-microspheres, Inflammation, Angiogenesis.

1. Introduction

In recent years, the development of nanostructures formed by a low or limited number of atoms has been escalating due to the unusual properties of these systems; whilst, at the same time, raising several problems in connection with their structural stability. An alternative method, which has been recently introduced, consists in anchoring specific nanoparticles on top of certain surfaces, not undermining but instead improving their physicochemical properties. At present, this can be catalogued as one of the most exciting challenges in relation with the engineering of modern nanomaterials; the properties of which can be modulated not only on the basis of the particular natures of their constituting units, but also by tuning the distance between nanoparticles or by regulating the morphology of the nanoparticles. The control of particle size and morphology enables certain flexibility in such a way as to generate new types of nanostructures, which allow a

*Corresponding author: luisaojedam@yahoo.com.mx

good choice of the intrinsic physical and chemical properties. Having this objective in mind, the intervention of silica (SiO_2) particles during the course of biological processes has been recently reported, as for instance, in immune system modulation [1, 2], fibrogenesis [3, 4], angiogenesis [5, 6], inflammation [7, 8], oxidative stress-cytotoxicity [9, 10], and others. Previously, diverse authors have reported the anchorage of metallic nanoparticles on top of SiO_2 structures [11-14]. Concerning to this last kind of systems, we have found that when attaining a high coverage of the surface of silica microspheres with silver nanoparticles (Ag^0NPs), this induces the SiO_2 particles to be more strongly attracted by their nearest homologous neighbors. This not only facilitates the silver nanoparticles to be anchored on top of the silica spheres but also to cause an aggregation of them, thus creating chains of Ag^0NPs up and down the SiO_2 microspheres. However, the optimization of this method of synthesis would still permit a higher concentration as well as a more homogeneous distribution of the Ag^0NPs , aspects that could make possible a better control of the structure of the final hybrid material.[15]

In the case of biomedical applications, several reports have suggested that silica can influence and modulate several factors related to tissue repair. This is the case of cytokine generation for collagen synthesis (scarring) [16], and the new vessels blood generation (angiogenesis)[5]. On the other hand, it has been demonstrated that silver exerts important beneficial effects on wound healing due to its antimicrobial properties [17], while at the same time stimulating other unknown step pathways during skin repair processes. Similarly, Ag can result in the obtaining of better mechanical tissue properties(i.e. collagen alignment) during wound healing. [18] Additionally, Ag^0NPs have been extensively investigated for the treatment of several pathophysiological alterations for hygienic and healing purposes [19, 20]. Due to the above-mentioned motivation, in this work, we describe a novel method for synthesizing Ag chains of nanoparticles on top of SiO_2 microspheres, this would allow employing the deposited Ag^0NPs as links between neighboring SiO_2 microparticles for their use in experimental skin wound healing.

2. Material and methods

2.1. Synthesis of colloidal silver nanoparticles, Ag^0NPs

Silver *sols* were prepared, from 0.1 g of silver nitrate (AgNO_3) dissolved in 100 mL of ethanol while employing polyvinyl-pyrrolidone (PVP) as the colloidal stabilizing agent, under a 1:10 weight ratio (i.e. with respect to Ag) and also adding one gram equivalent of magnesium metal shavings. The resultant mixture was maintained under reflux conditions at 363 K and subjected to constant stirring for a period of 12 h [21]. The formation of nanoparticles could be observed through a change in color of the reacting mixture, since small Ag^0NPs render a yellowish color. The addition of a tiny amount of PVP effectively prevented the mutual aggregation of Ag^0NPs . The presence of a colloidal suspension can be detected by the reflection of a laser beam from the particles. The most prominent absorption band of this colloidal suspension was located at 420 nm. This band is characteristic of the plasmon band exhibited by Ag^0 colloids. [22, 23]

2.2. Synthesis of SiO_2/Ag^0 microspheres.

The SiO_2/Ag^0 particles were prepared on the basis of the well-known Stöber method [24, 25], which consists in the base-catalyzed hydrolysis of tetraethoxysilane (TEOS). To perform this synthesis, an 11.9 M NH_3 aqueous solution, ethanol (88.1 mL), and 0.5 mL of a 5.224×10^{-3} M dispersion of Ag^0NPs , were mixed together and kept at 20°C; subsequently, a volume of 3.6 mL of TEOS was added, while the whole reacting system was subjected to strong magnetic stirring. In order to assure that the reaction had been completed, the mixture was gently stirred for further 15 h; after this time the solution remained undisturbed for 15 days. The resultant solid-liquid dispersion was centrifuged for 30 minutes at 3000 rpm and dried in an oven at 60 °C for 4 h. As reference material, pristine silica microspheres with no adhered Ag^0NPs was prepared by following the same procedure as previously described.

2.3. Characterization

The SiO₂ and SiO₂/Ag⁰ substrates were characterized via a FTIR Varian 660 Spectrometer. Samples were prepared in the form of KBr disks. The absorption spectra were measured with a Cary-300 UV-Visible spectrometer. Transmission Electron Microscopy (TEM) images were taken in a JEM-2010F FASTEM electron microscope operating at 200 kV; the samples used were first dispersed in isopropanol, next deposited on 300 mesh copper grids, and subsequently dried in air before being analyzed by TEM.

2.4. Wound healing experimental design

A total of 15 male Wistar rats weighing 180–200 g were selected for the study; each animal was individually housed and maintained on a normal food and water diet. The specimens were housed in the animal facility in the Bioterium of the University of Guadalajara and all animal studies were conducted in accordance to the principles and procedures outlined in the “Norma Oficial Mexicana” (Official Mexican Standard) Guidelines for the Care and Use of Laboratory Animals [26] and also under the Principles of the Manual Handling of Animals for Experimentation and Teaching.[27] Before performing the incision wound process, the dorsal fur of the animals was shaved with an electric clipper and anesthetized by means of ketamine (120mg kg⁻¹ body weight). Then, a longitudinal paravertebral incision of 1 cm in length was made through the skin on the back of each animal under sterile conditions. The wounds were left undressed and the animals were next randomly divided into three groups of five individuals each. Two testing groups of rats were applied 1.6 μg approximately of the SiO₂ or SiO₂/Ag⁰ nanostructures; afterwards, the individuals were evaluated along 12 post-skin surgery days. A control animal group with inflicted incisions but without treatment was also included in the study. A periodical evaluation was made for each experimental group in order to determine the extent of tissue recuperation along the duration of the study.

2.5. Histological analysis

Once the study finalized (12 days) the animals were anesthetized, sacrificed and a portion of skin tissue was taken for histopathological and immunohistochemical analyses. Briefly, the tissue was immersed for 5 min in *para*-formaldehyde (4%, pH 7.4) diluted in phosphate-buffered saline, dehydrated in graded ethyl alcohol and embedded in paraffin block. In turn, 5 μm thick skin sections were adhered and fixed in glass slides by silane treatments of slides and were subjected to Masson’s trichrome and Hematoxiline & Eosine (H&E) staining for determination of extracellular matrix proteins (scarring marker) and histo-architecture/inflammation of the tissue, respectively, in each experimental group. The histological analysis was made in 15 random fields in order to evaluate the amount of blood vessels, extracellular matrix deposits, as well as infiltrated inflammatory and fibroblastic cell presence.

Another set of skin sections was mounted in electrocharged slides Superfrost plus (Shandon Thermo Scientific) and deparaffinized by hot, the endogenous activity of peroxidase was quenched with 3.0% H₂O₂ in absolute methanol. Skin sections were incubated overnight at room temperature with mouse monoclonal IgG specific antibody against α-smooth muscle actin -α-SMA- (Abcam, Cambridge, MA) and proliferation cell nuclear antigen -PCNA- (Abcam, Cambridge, MA), to determine myofibroblasts and cell proliferation presence, diluted 1/50 and 1/100, respectively, in PBS. Bound antibodies were detected with peroxidase labeled rabbit polyclonal antibodies against mouse or goat immunoglobulins and revealed using diaminobenzidine as substrate and counterstained with hematoxylin. Histopathology was interpreted by two independent board certified pathologists who were blinded to the study.

3. Results

The SiO₂/Ag⁰ systems were synthesized in our laboratory, through the versatile *soft* chemistry or sol-gel procedure, which made possible to tune up the sizes of Ag nanoparticles in the interval of 1- 9 nm and of the silica spheres in the range of 200-300 nm.

3.1. Spectroscopic characterization

In the respective UV-Vis spectra of SiO_2 and SiO_2/Ag^0 samples shown in Fig. 1, the absorption peaks therein observed are due to the surface plasmon resonance (SPR) of the SiO_2/Ag^0 nanoparticles. The SiO_2/Ag^0 SPR signal appears at 426 nm, something that is consistent with silver nanoparticles SPR emission. [22, 23] This band is induced by the coupling between the oscillation of the electron cloud on the surface of the Ag^0 NPs and the incident electromagnetic wave in quasi-static regimen. The SiO_2 matrix shows no characteristic absorption peak in the 200-800 nm wavelength range.

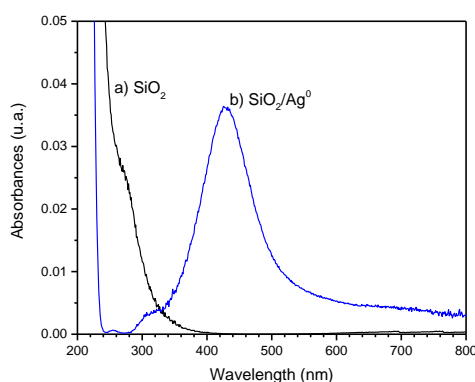


Fig. 1. UV-Vis of SiO_2 and SiO_2/Ag^0 microsphere substrates

The FTIR spectra of SiO_2 and SiO_2/Ag^0 specimens (Fig. 2) show peaks at 1630, 3400, and 3600 cm^{-1} due to O-H vibrations, which can be associated to remnant

Si-OH surface groups alone or interacting with physisorbed water molecules on the pore walls of these materials. The peak corresponding to the Si-O stretching vibration of Si-OH bonds appears between 954 and 810 cm^{-1} ; in turn, the Si-O-Si band appears from 1000 to 1130 cm^{-1} . [28] Additionally, the SiO_2 bands at 465 cm^{-1} can be due to Si-O-Si or O-Si-O species and this same signal is shifted to 473 cm^{-1} for the SiO_2/Ag^0 specimen. Additionally, Ag^0 NPs stretching bands appear from 500 to 550 cm^{-1} . However, Ag-O-Si bonds are not observed; furthermore, the splitting and shifting of the bands observed for SiO_2/Ag^0 indicate the formation of the above bonds. [29, 30].

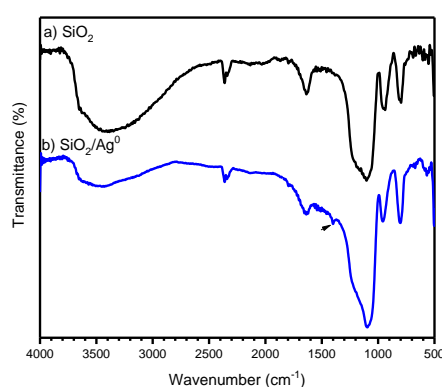


Fig. 2. FTIR of the SiO_2 and SiO_2/Ag^0 microsphere substrates.

3.2. Microscopic characterization

The HRTEM images displayed in Fig. 3a show some of the spheres composing an amorphous SiO_2 matrix, which are supporting the Ag^0 NPs, as evidenced by the corresponding bright and dark field images. In all samples, a partial aggregation of SiO_2 particles occurred; initially, Ag^0 species forms irregularly shaped clusters composed of single nanocrystals (of about 2-8 nm) resting on top of the silica surface. These aggregates are held together along an irregular

porous network. It should be pointed out that the decomposition of the precursory AgNO_3 salt and the successive formation and deposition of Ag^0NPs on top of the silica surface are fairly fast processes. The particles are quite uniformly arranged on the surface of the silica spheres and have a nearly spherical shape. Remarkably, there is almost no change in the mean particle size and coverage of the silica surface from one to another sample. Ag^0NPs entrapment occurs in the silica matrix together with its adsorption on the external surface of the SiO_2 spheres

The statistical size analysis of Ag^0NPs reveals a mean diameter of about of 3 nm; as can be seen in the particle size distribution histogram shown in Fig. 3b, the size distribution of the sample is not following the behavior predicted by the Plasmon bandwidth. The final size and shape of the metal particles depend on the extent of the nucleation, growth, and interaction with the PVP-stabilizing agent.

Energy-dispersive spectroscopy (EDS) analyses of both pristine and Ag-doped SiO_2 matrices are shown in Fig. 3c. These images not only confirm the existence of Ag^0NPs on top of silica spheres, but also reveal the presence of other elements: i.e. those associated with the supporting silica spheres (Si and O) and peaks related to C, Cu, and Ag. While these data reiterates that the pore walls pertain to the SiO_2 nanospheres, the presences of Cu and C are due to the carbon-coated copper grids, which was the HRTEM substrate support that was utilized. Obviously, the Ag signal is caused by the Ag^0NPs .

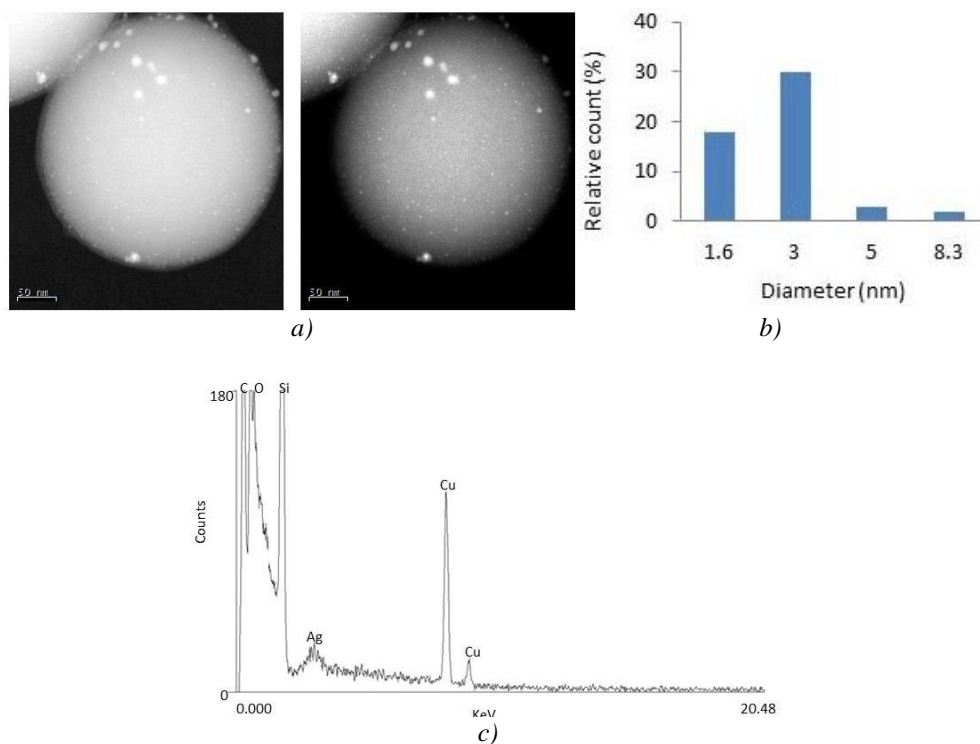


Fig. 3. HRTEM and EDS analyses of the amorphous SiO_2 matrix embedded with nanometric particles of silver bright field image. Additionally, images show the Ag^0NPs size

The above results gives a hint about that the interaction of Ag^0NPs with the surface groups of the silica substrate inhibits the mutual aggregation of these nanospheres; the main reason for this to happen should be due to the steric protection provided by PVP around the SiO_2 globules. This stabilization contrasts with what happening when metal or metal oxide nanoparticles are synthesized from alternative methods, as for instance, those consisting in the reduction of silver cations to silver by employing assorted compounds. This last procedure promotes a controlled aggregation of Ag particles, thus reaching sizes that result inadequate for specific applications, especially those requiring particle sizes smaller than 10 nm. Importantly, the attachment of Ag^0NPs on the surface of an inert solid renders a substrate adequate for diverse applications, such

as the one herein pursued. The controlled growth, aggregation, and homogenous repartition of Ag⁰NPs over the surface of the silica microsphere support make these materials prone to different applications, such as the creation of effective antibacterial and wound healing agents.

3.3. Wound healing activities

The skin repairing actions of each rat group treated with SiO₂ and SiO₂/Ag⁰ systems had a similar effect on tissue recuperation; nevertheless, the animals treated with SiO₂/Ag⁰ showed an important increment of hair growth in the damaged area (Fig. 4).



Fig. 4. Macroscopic image of skin injury in each experimental group during 12 days of treatment

This characteristic was corroborated during the histological analysis made after Masson's staining, where an increase in hair follicles was observed for the above mentioned group (Figs. 5A-C). The animals treated with pristine SiO₂ similarly showed the occurrence of this characteristic, although in a lesser extent. Additionally, an important decrement in the presence of extracellular matrix cells (blue color) was observed; an increment of healthy tissue (red color) with an abundant presence of blood vessels if compared against the scarce number of them existing in control, pristine SiO₂, and SiO₂/Ag⁰ groups. The abundance of cell infiltrate can be appreciated in the images shown in Fig. 5D-F (H&E), in which a pronounced decrement of these cells was only observed in those animals treated with SiO₂/Ag⁰. Furthermore, the epithelial thickness was thinner in this same group. A marked increment of α-SMA⁺ cells was observed in specimens treated with SiO₂/Ag⁰ (Fig. 6).

Interestingly, these cells were located around blood vessels, in congruence to those observed in Fig. 5, which resulted to be the most abundant ones. Finally, a notable increment of both epidermal and endodermal cell proliferation (PCNA⁺) was determined for tissue samples proceeding from the SiO₂/Ag⁰ treated animals, an effect that is clearly indicated by the brown color appearing in Fig. 7.

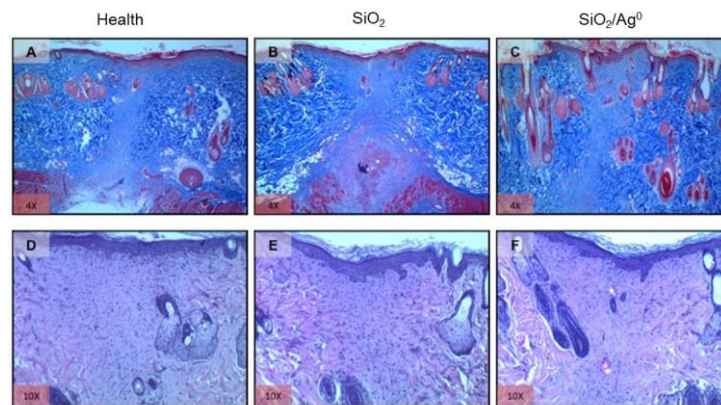


Fig. 5. Histological analysis by Hematoxiline-Eosine and Masson staining for each experimental group.

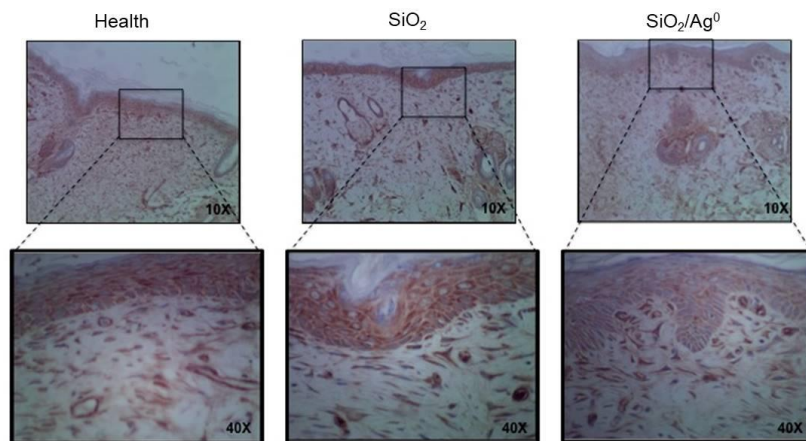


Fig. 6. α -SMA⁺ cells:immunohistochemical evaluation

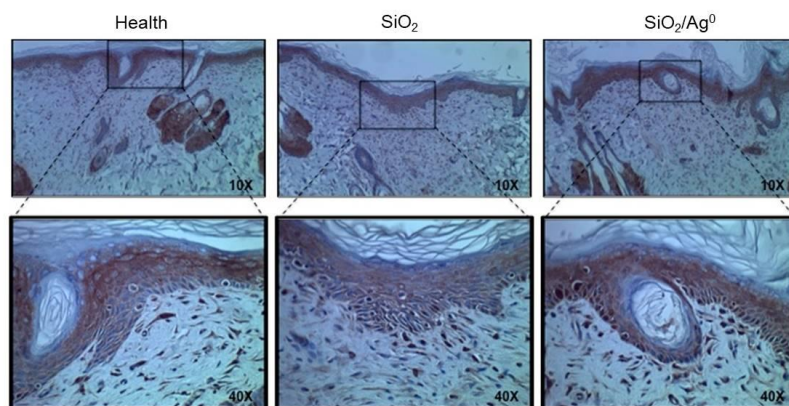


Fig. 7. PCNA⁺ cells:immunohistochemical evaluation.

4. Discussion

The evolution process occurring during skin wound healing involves dynamic, interactive mechanisms characterized by several precursory growth factors of cells and extracellular matrix

(synthesis/degradation). These processes are related to inflammation, cell proliferation, and extracellular matrix remodeling [30]. At this respect, several experimental therapeutic alternatives have been developed in which the use of nanotechnology for skin wound healing has been showing promising results. [20, 32, 33] Within this new technology, silica nanoparticles (SiO_2) have been employed in various fields, such as drug delivery devices, cosmetics, varnishes, additives for foods and, recently, in biomedical and biotechnological areas. [2] Diverse silica-based ceramics, which are mechanically strong, have been employed in several pathologies related to bone regeneration. For example, during head or mandibular traumatism silica, in combination with chemical molecules, as for instance silver nitrate [34], stimulates the resistance to bacterial infection while incrementing both cell proliferation and differentiation during bone regeneration. [35] On the other hand, a mixture of silicon and calcium, [36] improves both gene expression and biological performance. Interestingly, silica enhances the synthesis of type I collagen and alkaline phosphate [37]; both of these processes related to different routes aiming for tissue regeneration of bone and/or skin. Previously, our research group has reported the antimicrobial effects of SiO_2 plus Ag NPs, with promising results. [13] Similarly, other authors demonstrated that SiO_2/Ag^0 materials have antifungal properties on *Candida albicans* cells [38] or antibacterial (*Escherichia coli*) effects on wound covers, including an exploration with respect to the reusability of this material. [39]

In the present study, SiO_2 microspheres, plus Ag^0 NPs deposited on their surface, improve the healing process of full-thickness wounds during 12 days of post-treatment. As it was observed, treatments including either pristine SiO_2 or SiO_2 -Ag NPs had an important healing effect on wounds inflicted in animals; however, the best results were observed for SiO_2/Ag^0 systems, in which animals were characterized by an increment of hair follicles, something that was not previously reported by other authors: Additionally, there arose an important decrement of inflammatory cell presence, thus indicating an advanced state of tissue reparation. At the histological level, a significant decrease of extracellular matrix, as well as abundant blood vessels, were observed for the SiO_2/Ag^0 treated rat group, something which suggested that the injured area presented a more advanced state of reparation (remodeling). This agrees with what Ma, *et al.* has previously reported when stating that SiO_2 could induce the gene expression of MMP-9 (*i.e.* the direct effect or of extracellular matrix remodeling into an advanced state of tissue reparation) in alveolar macrophages. [3] Recently, our research group showed the good effect of Ag^0 NPs on skin wound healing and observed positive effects during the healing process in terms of increments in the collagen synthesis and fibroblast presence. [40] As, Reffitt *et al.* found, that SiO_2 has the capacity of increasing the rate of collagen synthesis (*i.e.* the most abundant of extracellular matrix protein). [37]

On the other hand, in relation to silica, recent studies have revealed that the 45S5 bioactive glass (a group of surface-reactive ceramic glasses with 45wt% SiO_2) could significantly stimulate an increment in the secretion of angiogenic growth factors, both *in vitro* and *in vivo*. [41] Similarly, several reports indicated an important gene expression rate of the basic fibroblast growth factor and vascular endothelial growth factor (bFGF and VEGF, respectively) that stimulates the proliferation of fibroblast and endothelial cells, thus promoting angiogenesis and wound healing. [42, 43] From our part, our results reveal an important presence of blood vessels after treatments with either pristine SiO_2 or SiO_2/Ag^0 substrates; consequently, we think that this effect can be due to the presence of Ag^0 NPs, as we have previously realized in a different study. [40]

Concerning angiogenesis, several studies have revealed that silica induces positive effects, such as those already indicated by Day *et al.* These authors have already found that the 45S5 bioactive glass can significantly stimulate the secretion of angiogenic growth factors both *in vitro* and *in vivo*, [41, 44] Additionally, this group of authors assume that by taking into count the wound closure rates found in their experiments, the best healing effect was partly caused by growth factors (*i.e.* bFGF and VEGF) stimulated by the 45S5 bioactive glass. [42]

Several authors have reported positive effects of AgNPs on cell proliferation of fibroblast and keratinocytes during skin wound healing; these results are in agreement to those reported by Tian *et al.*, and Liu X *et al.* authors that found important positive effects of AgNPs on the proliferation of several cells, such as fibroblasts and keratinocytes, during the skin wound healing process. [20, 45] As our results have shown, an important presence of proliferating cells (PCNA^+),

mainly in the epithelial zone, was observed in animals that received treatments with pristine SiO₂ spheres; however, this effect was the most intense in those animals which received SiO₂/Ag⁰. The above mentioned evidence demonstrates the positive effects of applying a combined nanostructured system, such as silica spheres with adhered Ag⁰NPs, as a promising substrate for providing an effective and straightforward treatment for diverse affections.

5. Conclusions

The results herein presented have shown the deposition of Ag⁰NPs (1.6-3 nm) on top of SiO₂ spheres of 2-12 nm in diameter; these systems depict an intense FTIR emission band at 426 nm. This fact suggests that the Ag⁰NPs anchored on neighboring spheres interact with each other, thus allowing a close approximation between them, which promotes the creation of chains of silica spheres on top of the silica particles, something that also provokes the approximation between SiO₂ nanospheres. The reaction mechanism is similar to that happening when silver particles are deposited on top of isolated nanospheres. As it was demonstrated here, the optimization of the respective method of synthesis of these systems allows reaching a high concentration and a homogeneous distribution of Ag⁰NPs along the surface of the silica globules then making possible the close approaching of silica spheres and the attainment of useful properties of the final hybrid materials. Additionally, it was observed that the treatment of skin with either SiO₂ or SiO₂/Ag⁰ substrates promotes an important healing effect on wounds surgically inflicted in laboratory animals; the best skin healing results were observed when employing SiO₂ plus AgNPs hybrid systems.

Acknowledgments

Thanks are given to PRODEP Academic Network "Nanoscope Design and Textural Properties of Advanced Materials", Academic Body of Sciences, Nanomaterials and Condensed matter UDG-CA-583, Academic Body of Physical Chemistry of Surfaces UAM-Iztapalapa CA-31, and finally to the Bioterium of the University Center for Health Science, University of Guadalajara. Thanks are also due to Patricia Castillo for her skilled technical assistance in the SEM-EDS experiments.

References

- [1] W. Wu, G. Mao, C. Yu, *Zhonghua Lao Dong Wei Sheng Zhi Ye Bing ZaZhi*, **20**(6), 455 (2002).
- [2] Eun-Jeoung Yang, In-Hong Choi, *Immune Network* **13**(3), 94 (2013).
- [3] X. B. Ma, X. L. Li, S. X. Sun, F. Yang, *Zhonghua Lao Dong Wei Sheng Zhi Ye Bing ZaZhi* **23**(3), 203 (2005).
- [4] M. Riedel, J. Brinckmann, A. Steffen, S. Nitsch, B. Wollenberg, H. Frenzel, *Journal der Deutschen Dermatologischen Gesellschaft* **11**(5), 412(2013).
- [5] R. Detsch, P. Stoor, A. Grunewald, J.A. Roether, N.C. Lindfors, A.R. Boccaccini, *Journal of Biomedical Material Researchpart A*, **102A**, 4055 (2014)".
- [6] A. Ring, S. Langer, D. Tilkorn, O. Goertz, L. Henrich, I. Stricker, et al, *Eplasty* **28**, 504 (2010).
- [7] J. L. Kang, I. S. Pack, H. S. Lee, V. Castranova, *Toxicology* **151**, 81 (2000).
- [8] J. L. Kang, E. Womans, Y. H. Go, K. C. Hur, V. Castranova, *Journal of Toxicology and Environmental Health Part A*; **60**(1), 27 (2000).
- [9] X. Yang, J. Liu, H. He, L. Zhou, C. Gong, X. Wang, *Particle and Fibre Toxicology* **7**,1 (2010).
- [10] Hyun-Jeong Eom, Jinhee Choi., *Environmental Health Toxicology* **26**, 1 (2011).
- [11] M. Khosroshahi, M. S. Nourbakhsh, *Medical Laser Application* **26**(1), 35(2011).

- [12] G. Gu, J. Xu, Y. Wu, M. Chen, L. Wu, *Journal of Colloid Interface Science* **359**, 327 (2011).
- [13] M. L. Ojeda-Martínez, Yáñez-Sánchez 2, A, Zamudio-Ojeda, F.J. Gálvez-Gastelum, R. Machuca-González, C. Velásquez-Ordoñez, *Digest Journal of Nanomaterial and Biostructures* **8**(1), 409(2013).
- [14] X. Li, H. Wang, H. Rong, W. Li, Y. Luo, K. Tian, et al, *Journal of Colloid and Interface Science* **445**, 312(2015).
- [15] H. Ma, Y. Jiao, B. Yin, S. Wang, S. Zhao, S. Huang, F. Meng, *ChemPhysChem* **5**(5), 713(2004).
- [16] Puri N and Talwar A, *Journal of Cutaneous Aesthetic Surgery* **2**(2), 104(2009).
- [17] J. S. Kim, E. Kuk, K.N. Yu, J.H. Kim, S.J. Park, H.J. Lee, et al, *Nanomedicine* **3**(1), 95(2007).
- [18] K.H. Kwan, X. Liu, M.K. To, K.W. Yeung, C.M. Ho, K.K. Wong, *Nanomedicine* **7**(4), 497(2011).
- [19] T. Liu, X. Song, Z. Guo, Y. Dong, N. Guo, X. Chang, *Colloids and Surfaces B* **116**, 793(2014).
- [20] J. Tian, K.K. Wong, C.M. Ho, C.N. Lok, W.Y. Yu, C.M. Che, et al, *Chem Med Chem* **2**, 129 (2007).
- [21] S. Ayyappan, R.S. Gopalan, G.N. Subbanna, C.N.R. Rao, *Journal of Materials Research* **12**(2), 398 (1997).
- [22] J.A. Creighton, C.G. Blatchford, M.G. Albrecht, *Journal of the Chemical Society, Faraday Transactions* **275**, 790 (1979).
- [23] M. Kerker, O. Siiman, DS Wang, *The Journal of Physical Chemistry* **88**(15), 3168 (1984).
- [24] W. Stöber, A. Fink, E. Bohn, *Journal of Colloid Interface Science* **26**(1), 62 (1968).
- [25] T. Ung, L. M. Liz-Marzán, P. Mulvaney, *Langmuir* **14**(14), 3740 (1998).
- [26] Norma Oficial Mexicana NOM-062-ZOO-1999.
- [27] E. Falconi de la Fuente, L. García-Magaña, O. Marín-Reyes, R.M. Padrón-López, G. Rivas-Acuña, G. Vargas-Simón, Universidad Juárez Autónoma de Tabasco, 2010.
- [28] R.S. McDonald, *The Journal of Physical Chemistry* **62**, 1168 (1958).
- [29] B. Karunakaran, K.S. Nahm, R.N. Elizabeth, *Nanoscale Research Letters* **4**(5), 452 (2009).
- [30] J. Angelito-Banos, et al, *Journal of Sol-Gel Science and Technology* **30**(2), 89 (2004).
- [31] F. H. Epstein, A.J. Singer, R.A.F Clark, *New England Journal of Medicine* **341**, 738 (1999).
- [32] J.G. Leu, S.A. Chen, H.M. Chen, W.M. Wu, C.F. Hung, Y.D. Yao, et al, *Nanomedicine* **8**(5), 767 (2012).
- [33] J.E. Kim, J. Lee, M. Jang, M.H. Kwak, J. Go, E.K. Kho, et al., *Biomaterials Science* **3**, 509 (2015).
- [34] Q.Z. Chen, I. D. Thompson, A. R. Boccaccini, *Biomaterials* **27**, 2414 (2006).
- [35] T. J. Webster, A. A. Patel, M. N. Rahaman, B. B. Sonny, *Acta Biomaterialia* **8**, 4447(2012).
- [36] M. Y. Shie, H. C. Chang, S. J. Ding, *International Endodontic Journal* **45**, 337 (2012).
- [37] D.M. Reffitt, N. Ogston, R. Jugdaohsingh, H. F. Cheung, B. A. Evans, R. P. Thompson, et al, *Bone* **32**, 127(2003).
- [38] M. Qasim, B.R. Singh, A.H. Naqvi, P. Paik, D. Das, *Nanotechnology* **26**(28), 285102 (2015).
- [39] M. Zhijun, J. Huijiao, T. Dezhi, T. Yu, D. Guoping, Z. Jiajia, et al, *Colloids and Surfaces A* **387**, 57 (2011).
- [40] M. L. Ojeda-Martínez, I. Yáñez-Sánchez, C. Velásquez-Ordoñez, M. M. Martínez-Palomar, A. Álvarez-Rodríguez, M. A. Garcia-Sánchez, et al, *Journal of Bioactive and Compatible Polymers* **30**(6), 617(2015).
- [41] H. Keshaw, A. Forbes, R.M. Day, *Biomaterials* **26**(19), 4171(2005).
- [42] Cong Mao, Cai Lin, Xiaofeng Chen, *Journal of Wuhan University of Technology-Mater Sci* **29**(5), 1063(2014).
- [43] P. Gerwins, E. Idenberg, L. Claesson-Welsh, *Critical Reviews in Oncology/Hematology* **34**(3), 185 (2000).
- [44] R. M. Day, *Tissue Engineering* **11**(5-6), 768(2005).
- [45] X. Liu, P.Y. Lee, C.M. Ho, V.C. Lui, Y. Chen, C.M. Che, et al., *Chem Med Chem* **5**, 468 (2010).